Vibrational properties of Si/Ge superlattices incorporating biatomic sheets of silicon and germanium

J. D. White,* G. Fasol,* and R. A. Ghanbari†
Cavendish Laboratory, University of Cambridge, Madingley Road, Cambridge CB3 0HE, United Kingdom

M. A. Gell, C. J. Gibbings, and C. G. Tuppen
British Telecom Research Laboratories, Martlesham Heath, Ipswich IP5 7RE, United Kingdom
(Received 15 May 1990; revised manuscript received 4 September 1990)

We find that the incorporation of a biatomic sheet of either Si or Ge into a Si/Ge short-period superlattice gives rise to a distinctive Raman spectrum in the wave-number range 370–410 cm^{-1}. We prove that this signal is due to the interfaces of the superlattice and originates from phonon modes within the superlattice, which should not normally be observed in the scattering configuration employed. As symmetry arguments, supported by detailed three-dimensional modeling, preclude the effect from being seen in structures with monatomic or triatomic sheets, we propose that the Raman line shape can be used as a sensitive tool to detect the presence of biatomic sheets of Si in Si/Ge superlattices.

INTRODUCTION

Over the last few years there has been a great effort to make Si-based devices emit light. The method widely adopted incorporates Si into a superlattice structure with germanium.[1,2] Recently it has been theoretically predicted that [001]-oriented superlattices which incorporate a biatomic sheet of silicon are promising candidates to emit luminescence.[3,4] The candidate structures have the form $(Si)_2/(Ge)_n$, where $6 \lesssim n \lesssim 10$ and are centrosymmetric and have space-group symmetries D_{2h}^5 ($Pmma$), D_{2h}^{28} ($Imma$), and D_{4h}^{19} ($I4_1/amd$). The present work investigates these and related superlattices grown on (001) Si and Ge substrates using Raman spectroscopy, which is an extremely useful method of structural and electronic characterizations.[5–7] In this work we use Raman spectroscopy to probe the phonon modes of the superlattice. We find a distinctive Raman signal that arises unambiguously from the presence of a biatomic sheet within the structure.

In a Si/Ge superlattice, both the nature and number of phonon modes are different from either bulk Si or bulk Ge. The multiplicity of modes arises from the superperiodicity of the structure and the novel characters of the modes are a consequence of compositional modulation. Depending on selection rules, some of these modes can be detected in Raman-scattering measurements.[8] Si/Ge superlattices are particularly suitable for Raman investigations as such structures are three-mode-vibrational systems: There are Si-Si, Ge-Ge, and Si-Ge vibrations derived, respectively, from the Si layers, the Ge layers, and the interfaces of the superlattice. Each of the sets of vibrations gives rise to a separate set of peaks in the Raman spectrum. This is in contrast, for example, with the GaAs/AlAs superlattice system, which is a two-mode system and has only Ga-As and Al-As vibrations.[9] We use a combination of three-dimensional modeling and Raman measurements to investigate the consequences of the presence of biatomic sheets of Si or Ge in a Si/Ge superlattice.

METHOD

The superlattices were grown by Si/Ge molecular-beam epitaxy (MBE). Growth was carried out in a Vacuum Generators VG Semicon V80 Si MBE system, equipped with Airco Temescal electron-beam evaporators and an Inficon Sentinel III flux control system. For growth on Si substrates, the native oxide was removed from Wacker (001) substrates held at 850 °C with a silicon flux of 1.5×10^{14} atoms $cm^{-2}s^{-1}$. For growth on Ge substrates, Ge(001) wafers, supplied by Hoboken and Mitsui, were heated to 780 °C for 5 min to desorb the surface oxide. Then, for both Si and Ge substrates, the temperature was lowered to 300 °C–500 °C for growth of the superlattice at 0.3-0.5 Å/s. The Raman measurements were made using various lines of a Kr^+ laser and performed in the $Z(XY)\bar{Z}$ configuration, where $\mathbf{X}\|[100]$, $\mathbf{Y}\|[010]$, and $\mathbf{Z}\|[001]$. The samples were kept at 77 K on the cold copper finger of a cryostat cooled with liquid N_2. The spectra were all taken with a DILOR XY multichannel Raman system.

On the theoretical side, the model that we used was based on a six parameter valence-force-potential method.[10,11] Since the model is three dimensional, it is possible to calculate the phonon dispersions for all directions in wave-vector space, although the selection of results presented here is only for the growth direction (defined as the $\Gamma-Z$ direction).[12]

THEORETICAL RESULTS

The configuration of a (001) biatomic Si sheet is shown in Fig. 1. Si atoms in both atomic layers "see" Ge atoms on one side. From previous calculations, it has been

shown that the presence of the third-bond type, i.e., Si—Ge bonds, at the interfaces between the Si and Ge layers, leads to two transverse modes that are localized to the interfacial region.[13] If the superlattice is of symmetry D_{2h}^{5}, D_{2h}^{28}, or D_{4h}^{19}, then these interfacial modes have an energy splitting, the magnitude of which is determined by the thickness of the Si and Ge layers.[11] It is found that the splitting reaches a maximum when the superlattice contains a biatomic sheet of Si or Ge. The splitting is substantially reduced when both the Si and Ge layers have their thicknesses increased. This suggests that the magnitude of the splitting is dependent on the proximity of the interfaces and a cross-coupling mechanism.

The phonon dispersions in the growth direction of a $(Si)_2/(Ge)_2$ superlattice grown on a (001) Si substrate are shown in Fig. 2(a). The displacements of the two transverse modes are shown in Fig. 2(b). This structure is the smallest-period Si/Ge superlattice with D_{2h}^{5} space-group symmetry and exhibits the maximum interfacial coupling. The two interface modes are shown in the spectrum of transverse modes at 372 and 419 cm^{-1}. From the corresponding displacement patterns, the modes exhibit symmetric and antisymmetric behavior at either interface. For all the cases presented here, the antisymmetric mode is of higher energy.

In Fig. 3 we show the calculated phonon dispersions for a $(Si)_2/(Ge)_6$ superlattice grown on a (001) Ge substrate, along the $\Gamma-Z$ direction; this dispersion can be compared with the dispersion shown in Fig. 2. The longitudinally and transversely polarized phonons are plotted separately. In the longitudinal polarization there are more modes in the region of 300 cm^{-1} due to confined optical modes in the thicker Ge layer. From 400 to 520 cm^{-1}, the band structure is very similar to that shown in Fig. 2 because the modes in this range are due to the Si layer, which has not changed. In the transverse polarization there are two modes, which, at the zone center, are

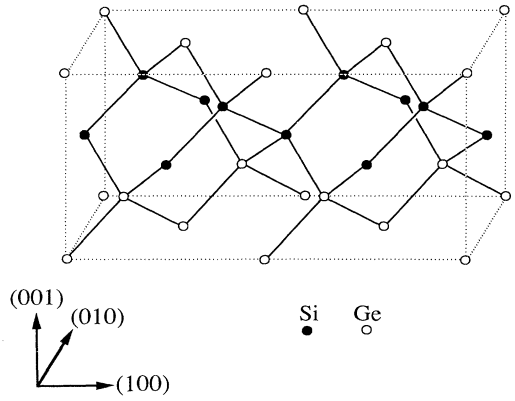

FIG. 1. Geometry of a biatomic sheet of Si. Shown are two bulk fcc cells with the atoms that comprise the biatomic sheet shown as solid circles. If the biatomic sheet was composed of Si and grown on a Ge substrate, the sheet would be stretched slightly in the in-plane direction as it takes up the lattice constant of the surrounding Ge layers.

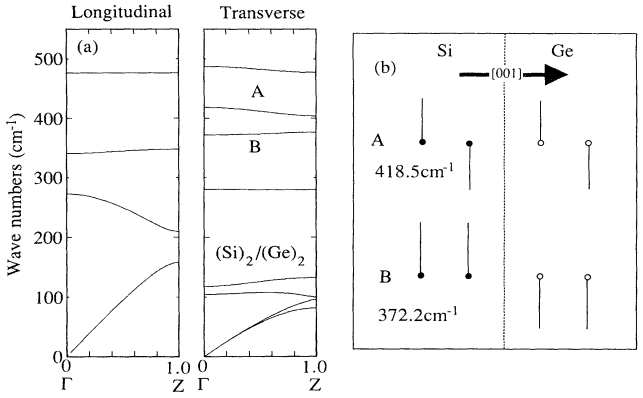

FIG. 2. (a) $\Gamma-Z$ dispersions for a $(Si)_2/(Ge)_2$ superlattice on a (001) Si substrate. The longitudinal and transverse branches have been selected and plotted separately. The two transverse interface modes, *A* and *B*, are shown at 372 and 419 cm^{-1}, respectively. Their displacement pattern is shown in (b), each circle representing the motion of an atomic sheet. Note that the two modes show symmetric and antisymmetric behavior with respect to each other with the antisymmetric mode, mode *A*, at 419 cm^{-1}.

split by approximately 30 cm^{-1}. The splitting is reduced from the case of the $(Si)_2/(Ge)_2$ because the interfacial cross-coupling through the thicker Ge layer is now substantially reduced; the coupling is almost monolateral.

EXPERIMENTAL RESULTS

Figure 4(a) shows the Raman spectrum of a $(Si)_2/(Ge)_6$ superlattice grown on a (001) Ge substrate.

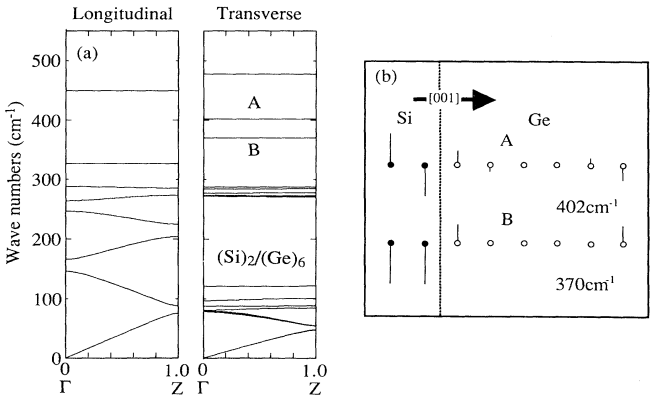

FIG. 3. (a) $\Gamma-Z$ dispersions for a $(Si)_2/(Ge)_6$ superlattice on a (001) Ge substrate. The longitudinal and transverse branches have been selected and plotted separately. The two transverse interface modes, *A* and *B*, have now moved closer together, because of the reduced coupling through the Ge layer, and are at 370 and 402 cm^{-1}. Their displacement pattern is shown in (b). Note that the two modes again show symmetric and antisymmetric behavior with respect to each other, with the antisymmetric mode, *A*, at 402 cm^{-1}.

The large peak at 304 cm^{-1} is due to the bulk LO phonon of the Ge substrate. The features below 300 cm^{-1} are caused by the confined phonons in the Ge layers of the superlattice. The peak at 390 cm^{-1} is from the interfaces of the superlattice. The broad peaks above 400 cm^{-1} are due to modes in the Si layer. The feature at 380 cm^{-1} is shown in more detail in Fig. 4(b). It has a double-peaked structure with a peak splitting of about 10 cm^{-1}. To exclude the possibility that the signal is from the substrate or the pseudomorphic growth on a Ge substrate, the Raman spectrum for an epitaxial layer of a pseudomorphically strained $Si_{0.25}Ge_{0.75}$ alloy on a (001) Ge substrate is shown in Fig. 5(a); the region around 380 cm^{-1} is expanded in Fig. 5(b). A broadly symmetric double-peaked structure is *not* observed in the alloy. Therefore, the double-peaked structure is associated with the superlattice. From Fig. 3, there are no longitudinal modes in the superlattice in the energy range 340–440 cm^{-1}. The only modes present are transverse interface modes, whose properties are dominated by the presence of the biatomic sheet of Si. If it is these modes that are the cause of the double-peaked structure, then the double-peaked structure in the Raman spectra should (with minimal bilateral coupling) remain unchanged as the thickness of the Ge layer is increased.

To test this hypothesis, samples with much thicker Ge layers were investigated. With thicker Ge layers, the relative concentration of the strained silicon decreases and the quality of the structure tends to increase. The superlattice investigated was a $(Si)_2/(Ge)_{21}$ superlattice on a (001) Ge substrate. Evidence from transmission electron microscopy (TEM) and x-ray rocking curves indicated that the sample was of excellent quality and had very-well-defined biatomic sheets of Si (see Table I). Figure 6(a) shows the Raman spectrum of the structure between 350 and 440 cm^{-1}. The double-peaked signal is again present. As a final test, a sample with 27 monolayers of

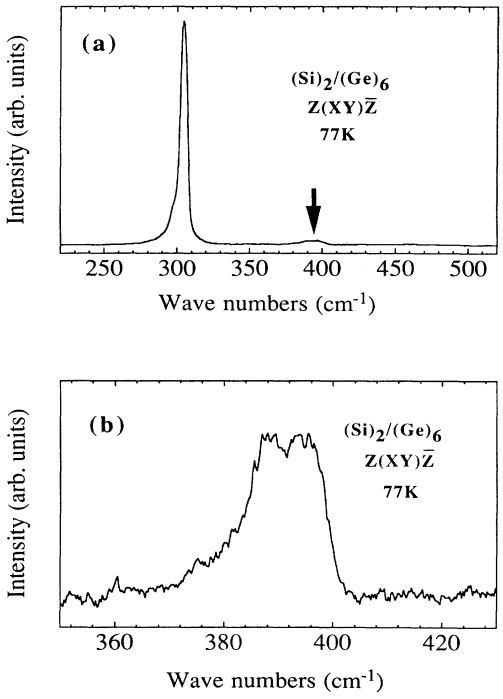

FIG. 4. (a) Raman spectrum of a $(Si)_2/(Ge)_6$ superlattice on a (001) Ge substrate. The spectrum was taken at an excitation wavelength of 5682 Å in a $Z(XY)\bar{Z}$ configuration with the sample at 77 K and held in vacuum. The large peak at 304 cm^{-1} is the bulk LO phonon from the substrate. The features that form the shoulder to this peak on the lower-energy side are due to confined modes in the Ge layers of the superlattice. The arrow at 385 cm^{-1} points to the interface mode that arises from Si-Ge vibrations at the interfaces of the superlattice. The region around 380 cm^{-1} is expanded in (b) and shows a distinctive double-peaked structure.

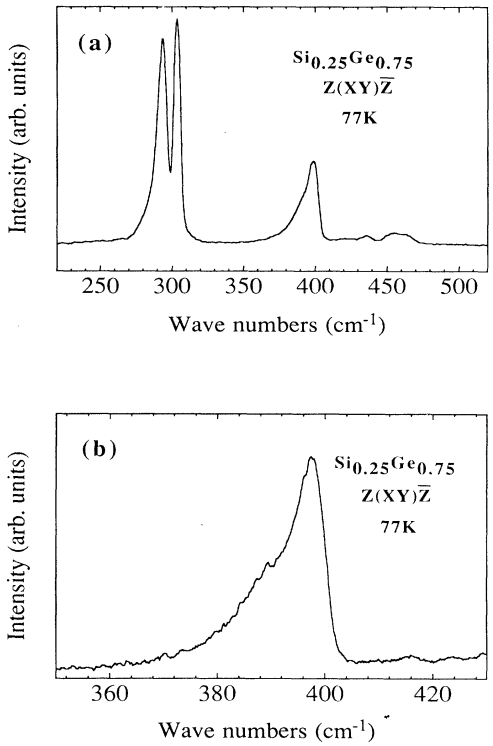

FIG. 5. Raman spectrum of a nominally $Si_{0.25}Ge_{0.75}$ coherently strained alloy layer on a (001) Ge substrate. X-ray diffraction indicated that the actual alloy concentration was $Si_{0.22}Ge_{0.78}$ and the relaxation in the layer was $\lesssim 5\%$. The spectrum was taken at an excitation wavelength of 5682 Å in a $Z(XY)\bar{Z}$ configuration with the sample held at 77 K in a vacuum. The large peak at 304 cm^{-1} is due to the substrate LO phonon. The Si-Ge mode is at 385 cm^{-1}. An expansion of the Si-Ge mode is shown in (b). The double-peaked signal present in the spectrum of the $(Si)_2/(Ge)_6$ superlattice is now absent. Therefore it is not associated with strained growth on Ge(001) substrates. To enable the x-ray measurements to be carried out, the sample was grown to a thickness 700 Å, so it was not an exact control structure for the $(Si)_2/(Ge)_6$ superlattice, which had a total thickness of ~ 100 Å. This makes the Raman signals from the alloy layer much stronger than the $(Si)_2/(Ge)_6$ superlattice Raman signals.

Ge in each period of the superlattice was investigated. The Raman spectrum for a nominally $(Si)_2/(Ge)_{27}$ superlattice on a (001) Ge substrate is shown in Fig. 6(b); investigation by x-ray diffraction reveals that this structure is actually $(Si)_{2.3}/(Ge)_{27.2}$ (see Table I). Again it has the same line shape as seen in the previous two samples. We can conclude from these measurements that the presence of a biatomic sheet in the superlattice gives rise to a characteristic double-peak shape for the Si-Ge mode of the superlattice; this characteristic line shape is independent of the Ge layer thickness.

If the complementary structure to a $(Si)_2/(Ge)_{21}$ is considered [i.e., a $(Si)_{21}/(Ge)_2$ superlattice], the biatomic sheet is of Ge. The calculated spectrum for a $(Si)_{20}/(Ge)_2$ superlattice is shown in Fig. 7(a). The transverse interface modes are at 386 and 395 cm^{-1} and their zone-center splitting is 9 cm^{-1}. This is compared with the modes in the $(Si)_2/(Ge)_{21}$, which have a zone-center splitting of $\sim$30 cm^{-1}. The experimental spectrum for the interface mode of a 40-period $(Si)_{20}/(Ge)_2$ superlattice on a (001) Si substrate is shown in Fig. 7(b). In the energy range 400–450 cm^{-1}, there is evidence for a double-peaked structure around the normal position of the interface mode seen in Si/Ge superlattices grown on Si substrates.

Since the selection rules forbid the observation of transverse modes in a backscattering Raman experiment off a (001)-oriented Si/Ge superlattice, some process must be relaxing the conditions and allowing the modes to be seen in the scattering configuration employed. The process is most probably related to interfacial disorder within the superlattice; no superlattice is perfect and modes with large amplitudes at the interface are most

TABLE I. Individual layer thicknesses derived from x-ray-diffraction studies, based on the [004] diffraction, for the larger-period superlattices. There are no data for the $(Si)_2/(Ge)_6$ superlattice, as the sample was not suitable for x-ray measurements.

Nominal structure $(Si)_m/(Ge)_n$	X-ray data m	X-ray data n	Figure in which the Raman spectrum is shown
$(Si)_2/(Ge)_6$			4(b)
$(Si)_2/(Ge)_{21}$	2.08±0.02	21.2±0.20	6(a)
$(Si)_2/(Ge)_{27}$	2.30±0.03	27.2±0.10	6(b)
$(Si)_{20}/(Ge)_2$	20.5±0.20	2.18±0.10	7(b)

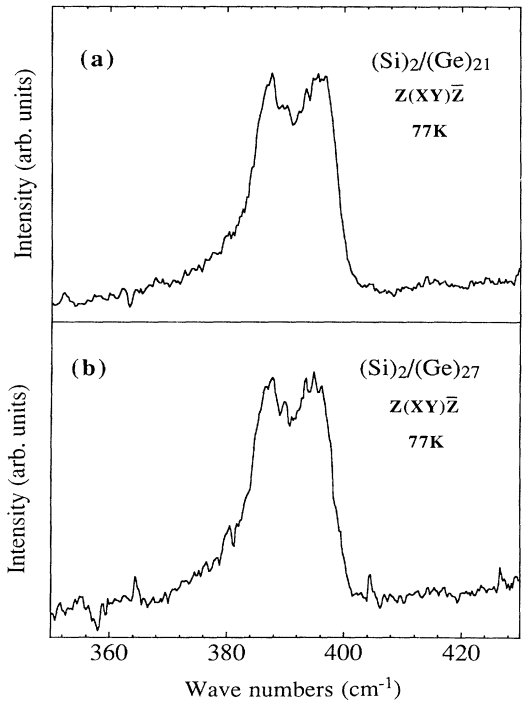

FIG. 6. (a) Raman spectrum of the interface mode of a $(Si)_2/(Ge)_{21}$ superlattice on a (001) Ge substrate. The spectrum was taken at an excitation wavelength of 5309 Å in a $Z(XY)\bar{Z}$ configuration with the sample held at 77 K in a vacuum. The peaks in the spectrum can be seen at 387 and 396 cm^{-1}. The double-peaked structure is far more pronounced in this structure. The Raman spectrum of the interface mode of a $(Si)_2/(Ge)_{27}$ superlattice on a (001) Ge substrate is shown in (b). The spectrum was taken at an excitation wavelength of 5682 Å in a $Z(XY)\bar{Z}$ configuration with the sample held at 77 K in a vacuum.

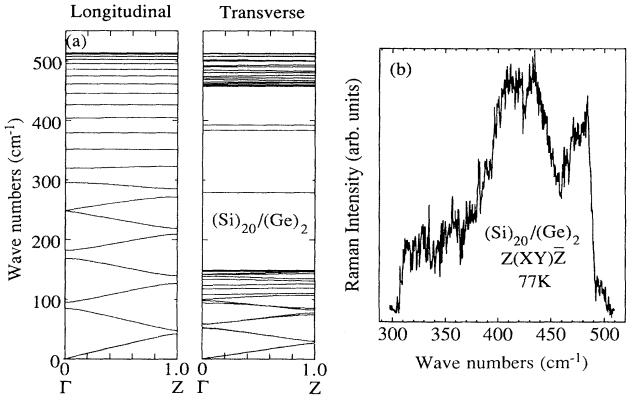

FIG. 7. Panel (a) shows the calculated $\Gamma-Z$ dispersions for a $(Si)_{20}/(Ge)_2$ superlattice grown on a (001) Si substrate. In longitudinal polarization, the ten highest-energy modes are the confined phonons in the Si layer. In transverse polarization, the modes above 450 cm^{-1} are the confined TO phonons in the Si layer. There is a pair of transverse interface modes around 390 cm^{-1} that are split by 9 cm^{-1}. The experimental spectrum of such a structure is shown in (b). The spectrum was taken at an excitation wavelength of 5309 Å in the $Z(XY)\bar{Z}$ configuration with the sample held at 77 K in a vacuum. There is a weak double-peaked structure at $\approx$425 cm^{-1}. At this excitation wavelength, the signal is substantially less than that from structures containing a biatomic sheet of Si, grown on Ge substrates. The low- and high-energy edges of the multichannel detector are at $\sim$ 310 and 490 cm^{-1}, respectively.

likely to exhibit disorder-induced scattering, which in this case are the higher-order-confined modes[14,15] and the transverse interface modes. It has been postulated that what is commonly called the interface mode in the Raman spectrum of a well-defined superlattice is actually a representation of the phonon density of states of modes localized at the interface.[13] In the energy range considered here, 370–410 cm^{-1}, it is postulated that the effects of the transverse interface phonons are being observed, with a broadening mechanism arising from non-zone-center phonons making a contribution to the Raman signal.

The discrepancy between the double-peaked splittings observed experimentally and those determined by calculation is about a factor of 3 for samples grown on Ge substrates. The theoretical splittings tend to be overestimated. For example, in the case of the $(Si)_2/(Ge)_{21}$ superlattice, the calculated splitting at the zone center is about 30 cm^{-1}, whereas the observed splitting [see Fig. 6(a)] is only 9 cm^{-1}. By carrying out full-zone density-of-states calculations, a symmetric double-peaked structure is produced, although the peak splitting is about 20 cm^{-1}. Thus contributions from density-of-states broadening reduces this discrepancy to a factor of 2. The origin of the difference is being investigated.

For transverse interface modes, the eigenfrequencies are determined to a large extent by the Si—Ge bond-force constant. It can be assumed that this frequency is similar to the eigenfrequency of Si—Ge bonds in a homogeneous pseudomorphic Si-Ge alloy system. If there is roughness present at the interfaces of an elemental superlattice, then, to first order, one period of a superlattice has the form $Si/Si_xGe_{1-x}/Ge/Si_xGe_{1-x}$, where the Si_xGe_{1-x} layers vary in thickness and concentration depending on the interfacial abruptness. The Raman peaks from the Si_xGe_{1-x} layers would be in the same energy range as the transverse interface modes that exist due to the layered nature of the superlattice. From the characterization data for the samples investigated in this work, both the Si and Ge layers are well defined. To take the specific example of the $(Si)_2/(Ge)_{21}$ superlattice, from Table I, x-ray-diffraction measurements have shown that the average composition of one period of the superlattice is $(Si)_{2.08}/(Ge)_{21.2}$. Cross-sectional TEM measurements have shown that the Si layers are in the form of well-defined biatomic sheets. So, in a first approximation, the excess Si atoms will be distributed above and below the Si layers, forming very dilute alloy layers at each interface. The resulting interfacial roughness will be sufficient to spoil the translational symmetry of the interface of the biatomic Si sheet, relaxing the backscattering Raman selection rules. But in this case, the number of extra Si—Ge bonds will be small ($\sim 8\%$), and so should not give rise to any significant Raman signal. For the $(Si)_2/(Ge)_{27}$ superlattice, the measured concentration for each period is found to be $(Si)_{2.3}/(Ge)_{27.2}$. The effective concentration of the alloy layers composed of the excess Si atoms at the interfaces is now substantially different from that of the previous sample, but from Fig. 6 it can be seen that the two samples have almost identical Raman line shapes. This provides evidence that the cause of the double-peaked structure in the Raman spectra is not due to alloying at the interfaces of the layers, but is due to the presence of the biatomic sheet of Si.

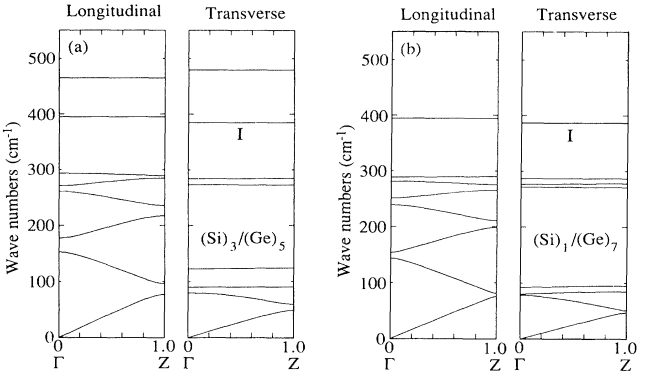

FIG. 8. (a) Calculated $\Gamma-Z$ dispersions for a $(Si)_3/(Ge)_5$ superlattice on a (001) Ge substrate. The interface modes at 385 cm^{-1} (labeled I) have collapsed onto a midway point and have become degenerate. (b) Calculated $\Gamma-Z$ dispersions for a $(Si)_1/(Ge)_7$ superlattice grown on a (001) Ge substrate. Again, the same phenomena are observed, with the two transverse modes becoming degenerate.

SYMMETRY EFFECTS

For Si/Ge superlattices, the possible space groups are D_{2h}^5, D_{2h}^{28}, D_{2d}^5 ($P\bar{4}m2$), D_{2d}^9 ($I\bar{4}m2$), D_{4h}^{19}, and T_d^2 ($F\bar{4}3m$) (Ref. 16). In this work, the *nominal* structures studied experimentally all have D_{2h}^5, D_{2h}^{28}, or D_{4h}^{19} space-group symmetry. For the case of the $(Si)_2/(Ge)_6$, which is a member of the D_{2h}^5 space group, all transversely polarized phonon branches are nondegenerate, in the $\Gamma-Z$ direction (Fig. 3). If a layer of Ge atoms is replaced by one of Si atoms, the space-group symmetry of the resulting $(Si)_3/(Ge)_5$ superlattice is D_{2d}^5. The $\Gamma-Z$ dispersions are shown in Fig. 8(a). The transverse-phonon branches have now formed doubly degenerate pairs. The interface phonons which previously had a splitting of 30 cm^{-1} have collapsed onto an energy that is roughly the average of the nondegenerate energies. A similar phenomenon occurs when a layer of Si atoms is replaced by a layer of Ge atoms, forming a $(Si)_1/(Ge)_7$ superlattice. The $\Gamma-Z$ dispersions for this structure are shown in Fig. 8(b).

The degenerate modes at 390 cm^{-1} in the $(Si)_3/(Ge)_5$ superlattice have a form similar to the nondegenerate modes in the $(Si)_2/(Ge)_6$ superlattice; that is, the largest displacement is located at the interface of the layers. The modes form a symmetric and antisymmetric pair, but have spatially orthogonal polarizations. The other major space group is D_{4h}^{19}. Superlattices of this space group can be obtained by adding a monolayer of Ge to a $(Si)_2/(Ge)_6$ structure, forming a $(Si)_2/(Ge)_7$ superlattice. D_{4h}^{19} structures in the [001] direction are a little different in that the unit cell contains two periods of the superlattice. It is found that the transverse interface modes change charac-

ter slightly, but still retain a similar energy splitting.[17]

It can be concluded from this that the presence of a biatomic sheet of Si (or Ge) will cause the presence of two nondegenerate transverse modes located at the interface of the layers in the superlattice, which have a significant energy splitting. For the case of the biatomic sheet of Si, it is found that the magnitude of the splitting, to a first approximation, is independent of the thickness of the Ge layer, for Ge-layer thicknesses of about 5 monolayers or greater. On the other hand, any significant deviation of the layer thickness from 2 monolayers is predicted to cause the splitting to disappear. The same behavior is predicted for a biatomic sheet of Ge embedded between layers of Si, although the magnitude of the energy splittings are calculated to be different.

As an aside, the calculations presented here show effects which must be taken into account when attempting to model Si/Ge superlattices using the one-dimensional linear-chain method. The linear-chain method has been used on many occasions to model the phonon dispersion curves in ideal (001) GaAs/AlAs superlattices.[18,19] All ideal (001) GaAs/AlAs superlattices have D_{2d}^5 or D_{2d}^9 space-group symmetry, depending on the relative number of monolayers in one period of the superlattice.[20] It is found that the [001] transverse-phonon branches in GaAs/AlAs superlattices are doubly degenerate[21] and, as pointed out above, this is also the case for Si/Ge superlattices with D_{2d}^5 or D_{2d}^9 space-group symmetry.[16] Therefore, phenomenologically, the degeneracy is characteristic of (001) superlattices with D_{2d}^5 or D_{2d}^9 space-group symmetry.[22] The basic linear-chain model has two force constants, one each for the longitudinal- and transverse-phonon branches, causing the transverse-phonon branches to be doubly degenerate.[18] Such a model can therefore be used for all perfect (001) GaAs/AlAs superlattices and Si/Ge superlattices with D_{2d}^5 or D_{2d}^9 space-group symmetry, such as the $(Si)_3/(Ge)_5$ structure. For Si/Ge superlattices with space-group symmetries of D_{2h}^5 or D_{2h}^{28} [such as the $(Si)_2/(Ge)_6$, space group D_{2h}^5] and D_{4h}^{19} [for example, the $(Si)_2/(Ge)_7$ superlattice], the degeneracies are lifted and a more complete set of force constants must be used,[23,24] in order that the correct energy splittings are predicted.

SUMMARY

We have used Raman scattering and a three-dimensional lattice-dynamical model to investigate Si/Ge superlattice microstructures. We have demonstrated a new interfacial phenomenon which gives rise to a characteristic double peak shape in the Raman spectrum of ultrashort-period Si/Ge superlattices that contain a biatomic sheet of Si. The effect may also be observable in Si/Ge structures that contain biatomic sheets of Ge. Further properties of these and other structures will be discussed elsewhere. This double-peaked Raman spectrum could usefully form the basis of a characterization method for direct-band-gap $(Si)_2/(Ge)_n$ structures. We have also elucidated phenomena associated with the superlattice space groups, which determine the set of parameters that have to be used when modeling Si/Ge superlattices with the one-dimensional linear-chain method.

ACKNOWLEDGMENTS

We would like to thank B. Jusserand for very useful discussions. We are indebted to J. Nicholls for critical reading of the manuscript. We would like to acknowledge the United Kingdom Science and Engineering Research Council and British Telecom for financial support. Another (R.A.G.) wishes to acknowledge the support of the Churchill foundation and the U.S. Office of Naval Research.

*Present address: Hitachi Cambridge Laboratory, Cavendish Laboratory, Madingley Road, Cambridge CB3 0HE, United Kingdom.

†Present address: Department of Electrical Engineering and Computer Science, Massachusetts Institute of Technology, Cambridge, MA 02139.

[1]U. Gnutzmann and K. Clausecker, Appl. Phys. **3**, 9 (1974).

[2]T. P. Pearsall, J. Bevk, L. C. Feldman, J. M. Bonar, and J. P. Mannaerts, Phys. Rev. Lett. **58**, 729 (1987).

[3]Michael Gell, Appl. Phys. Lett. **55**, 484 (1989).

[4]Michael Gell, Phys. Rev. B **40**, 1966 (1989).

[5]H. Brugger, E. Friess, G. Abstreiter, E. Kasper, and H. Kibbel, Semicond. Sci. Technol. **3**, 1166 (1988).

[6]E. Friess, H. Brugger, K. Eberl, G. Krotz, and G. Abstreiter, Solid State. Commun. **69**, 899 (1989).

[7]M. W. C. Dharma, G. C. Aers, D. J. Lockwood, and J. M. Baribeau, Phys. Rev. B **41**, 5319 (1990).

[8]M. Cardona, in *Light Scattering in Solids II,* edited by M. Cardona and G. Güntherodt (Springer-Verlag, Berlin, 1982), p. 45.

[9]B. Jusserand and M. Cardona, in *Light Scattering in Solids V,* edited by M. Cardona and G. Güntherodt (Springer-Verlag, Berlin, 1989), p. 49.

[10]R. A. Ghanbari, and G. Fasol, Solid State Commun. **70**, 1025 (1989).

[11]R. A. Ghanbari, J. D. White, G. Fasol, C. J. Gibbings, and C. G. Tuppen, Phys. Rev. B **42**, 7033 (1990).

[12]M. A. Gell and A. C. Churchill, Phys. Rev. B **39**, 10449 (1989).

[13]J. White, G. Fasol, R. A. Ghanbari, C. J. Gibbings, and C. G. Tuppen, Thin Solid Films **183**, 71 (1989).

[14]G. Fasol, M. Tanaka, H. Sakaki, and Y. Horikoshi, Phys. Rev. B **38**, 6056 (1988).

[15]E. Friess, K. Eberl, U. Menczigar, and G. Abstreiter, Solid State Commun. **73**, 203 (1990).

[16]M. I. Alonso, M. Cardona, and G. Kanellis, Solid State Commun. **69**, 479 (1989); **70**, i (1989) (erratum).

[17]J. D. White, R. A. Ghanbari, M. A. Gell, and G. Fasol (unpublished).

[18]B. Jusserand and D. Paquet, in *Heterojunctions and Semicon-*

ductor Superlattices, edited by G. Allan, G. Bastard, N. Boccara, M. Lannoo, and M. Voos (Springer-Verlag, Berlin, 1986), p. 108.
[19]E. Molinari, A. Fasolino, and K. Kunc, Superlatt. Microstruct. **2**, 397 (1986).
[20]M. Cardona, in *Spectroscopy of Semiconductor Microstructures,* edited by G. Fasol, A. Fasolino, and P. Lugli (Plenum, New York, 1989), p. 143.
[21]E. Richter and D. Strauch, Solid State Commun. **64**, 867 (1986).
[22]B. Jusserand (private communication).
[23]A. Fleszar and R. Resta, Phys. Rev. B **34**, 7140 (1986).
[24]E. Molinari and A. Fasolino, Appl. Phys. Lett. **54**, 1220 (1989).